

# COLLIMATED ELECTRON AND PROTON BEAM FROM ULTRA-INTENSE LASER INTERACTION WITH A REAR HOLE TARGET\*

X. H. Yang, Y. Y. Ma<sup>#</sup>, F. Q. Shao, T. P. Yu, Y. Yin, and C. L. Tian, Department of Physics, National University of Defense Technology, Changsha 410073, China

S. Kawata, Center for Optical Research and Education, Graduate School of Engineering, Utsunomiya University, 7-1-2 Yohtoh, Utsunomiya 321-8585, Japan

M. Y. Yu, Department of Physics, Institute for Fusion Theory and Simulation, Zhejiang University, Hangzhou 310027, China

Y. Q. Gu, Laser Fusion Research Center, China Academy of Engineering Physics, Mianyang 621000, China

H. Xu, National Laboratory Parallel and Distributed Processing, National University of Defense Technology, Changsha 410073, China

## Abstract

Collimated electron and proton beams from the interaction of an ultra-intense laser pulse with a rear hole target are studied by particle-in-cell (PIC) simulation. When an ultra-intense laser pulse irradiates on such a target, the hot electrons from the inner surfaces of the hole expand fast into the hole. However, the electrons at the corners expand slower and are compressed strongly. Then two intense electron jets as well as proton jets are sprayed out from the corners. The jets extend into the hole and focus along the laser propagation axis. The effects of the corner angle on the collimated proton beam are also investigated.

## INTRODUCTION

The generation of high current multi-MeV protons by ultra-intense short laser pulse irradiation thin target has been investigated [1-3]. The properties of the protons are of interest for a number of important applications, including particle accelerators [4], inertial confinement fusion [5], laboratory astrophysics [6], medical therapy [7], etc. However, because the proton beams are usually divergent and polyenergetic at the source, it is essential to reduce and control the proton beam divergence and energy spread for most applications.

In the past few years, much effort has been devoted to control the divergence of the proton beams. For example, Wilks et al. [8] showed that a target having a concave backside surface can result in more collimated and energetic protons by PIC simulation. Sonobe et al. [9] and Nakamura et al. [10] studied laser interaction with thin foils having a hole on the backside and obtained collimated proton beams by controlling the transverse profile of the electron cloud. Toncian et al. [11] presented a technique for focusing and energy selection of MeV proton beams with the use of transient radial electric fields on the inner walls of a hollow microcylinder, which

are triggered by an intense subpicosecond laser pulse. However, all these target profiles result in the divergence of the proton beams shortly after the focusing.

In this paper, we study the generation of focused and collimated electron and proton beams from a rear-holed target by the 2.5D PIC code PLASIM [12]. It is shown that two focused jets of high-energy electrons are ejected almost along the bisector of the inner corner angle which are tightly followed by two proton jets. Then they soon merge into a high quality collimated proton bunch. The bunch can propagate a relatively long distance in the hole cavity along the laser axis without divergence.

## SIMULATION MODEL AND RESULTS

In our simulations, the thickness of the target is  $5\lambda_0$ , the depth and diameter of the hole are  $7\lambda_0$  and  $8\lambda_0$ , respectively, where  $\lambda_0 = 0.8\mu\text{m}$  is the laser wavelength. The simulation box is  $60\lambda_0$  long and  $30\lambda_0$  wide. There are  $1024 \times 512$  grids, and  $6 \times 10^6$  particles per species. A p-polarized laser pulse is incident normally from the left boundary of the simulation box. The temporal and spatial (transverse) profiles are Gaussian, whose pulse width and spot radius are  $10T$  and  $10\lambda_0$ , respectively, where  $T$  is the light wave period. The peak intensity is  $I_0 = 5.0 \times 10^{19} \text{ W/cm}^2$ . The hydrogen target plasma has a density of  $10n_c$ , where  $n_c = 1.74 \times 10^{21} \text{ cm}^{-3}$  is the critical density. The initial temperatures of the electrons and protons are both 1 KeV. The lateral and left boundary conditions are periodic and Lindman-absorbing, respectively.

The target-front electrons are heated by the incident laser and pushed forward by the ponderomotive force as an intense laser pulse irradiates the target. These hot electrons can penetrate through the target and form an

\*Work supported by the National High-Tech ICF Committee, the National Natural Science Foundation of China (10976031 and 10975185), the Science and Technology Development Foundation of the Chinese Academy of Engineering Physics (2006Z0202), and the National Basic Research Program of China (2007CB815105). We also acknowledge the support of the National University of Defense Technology (NUDT) Foundation (JC09-02-08) and the NUDT High Performance Computer Research Center.

<sup>#</sup> plasim@163.com

electron cloud at the rear side. We present the electron and proton density distributions at the times  $t=269T$ ,  $377T$  and  $t=484T$  in Fig. 1. It's shown that after the high compression at the corners, two focused electron jets of electrons are emitted from the corners into the hole, which is almost along the bisector of the corner angle. Then, a strong space-charge field is generated near the inner corners, which accelerates the protons rapidly in the

target backside as in TNSA [8], except that here, because of the geometry and the corresponding field distribution, the protons emitted from the corner regions appear as beams that focus toward the axis. The physical mechanism is somewhat similar to what happened in typical armor-piercing shells due to the cumulative energy effect [13].

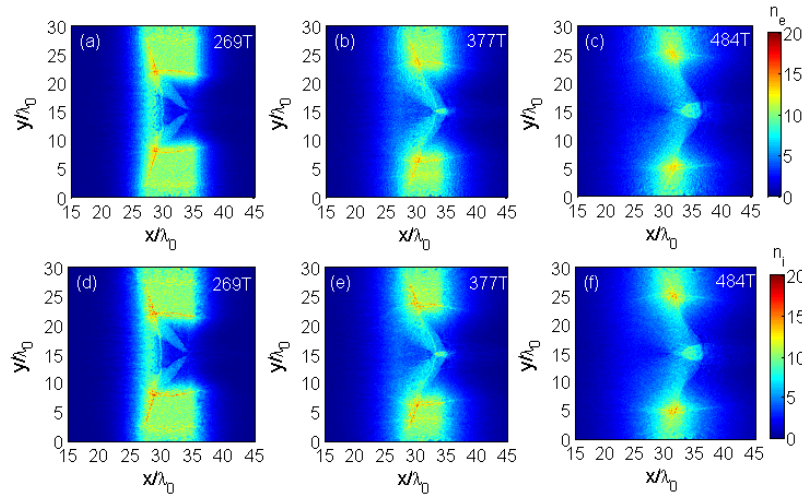


Figure 1: The density distributions of electrons (a, b, c) and protons (d, e, f) at  $t=269T$  (a, d),  $t=377T$  (b, e) and  $t=484T$  (c, f) for the target with angles of  $90^\circ$ , in units of  $n_c$ .

From Fig. 1 it is clear that more and more electrons are accelerated into the jets, so the diameter and density of the jets increase. It's also shown that the jets have changed their initial directions into the laser propagation axis as they converge on the axis. Eventually, the two jets merge at  $x \approx 33\lambda_0$ , where a single electron bunch with average density  $8.9n_c$  is formed. The accelerated protons also form jets whose evolution closely follows that of the electrons, as shown in Fig. 1 (d) and (e). The density of the proton bunch at the spot can reach  $8.85n_c$ . The collimated plasma bunch continues to move forward on the axis. From the snapshot of the plasma density distribution for some much later time, namely  $t=484T$ , as shown in Fig.1 (c) and (f), it can be seen that the bunch is continues being fed by more and more target electrons and protons, so its size increases with time. We investigate the transverse momentum distributions of the protons at the different time, and find that the transverse momenta of the protons in the hole are decreased with time, that is, the protons become more and more aligned to the axis.

In order to understand further the mechanism of the jet generation and obtain high a quality proton bunch, we consider the effects of the corner angles on the proton bunch properties, keeping other parameters same as before. The density distribution of the protons for the angle of  $60^\circ$  and  $120^\circ$  at  $t=269T$  and  $377T$  are presented in Fig. 2 and Fig. 3, respectively. Since the density distribution of the electrons has the same evolution as that of the protons, it is not given here. It can be seen that the proton jets are emitted almost along the bisector of the

corner angle, which is similar to the case of  $90^\circ$  angle. In this case the jets propagate much shorter distance before converge on the laser axis for the target with smaller angles. The larger the angle, the longer the focal length for the protons. For the target with angles of  $60^\circ$  most protons from the hole corners converge on the laser axis, which can also be seen in Fig. 4 (b). Fig. 4 shows that the proton density at the spot can reach  $11.34n_c$  for the  $60^\circ$  target, higher than that of  $90^\circ$  target at the time of  $377T$ , however, the current density is only  $1.07 \times 10^{12} A/cm^2$  much lower than that of the latter, which is  $1.24 \times 10^{12} A/cm^2$ . That means the kinetic energy of the proton bunch is lower for the  $60^\circ$  target, which also can be seen in Fig. 4(a). The protons cross the laser axis and are not efficiently accelerated in the laser axis direction for the target with smaller angle. From Fig. 3 and Fig. 4, we can see that for the target with  $120^\circ$  angles, the protons are accelerated more efficiently. However, the density of the proton bunch is much lower. It is because the focal length is too long for the protons emitted from the corners with larger angle. These protons will become dispersed before they merge so the density of the bunch is lower. Fig. 4(d) shows the angular distributions of the protons in the hole for the targets with different corner angles at the time of  $t=377T$ . It can be seen that the divergence angle of the protons is much smaller from the target with larger angle because the proton jets emitted almost along the bisector of the corner angle, and the angular distribution is to that of the flat target with the angle increasing.

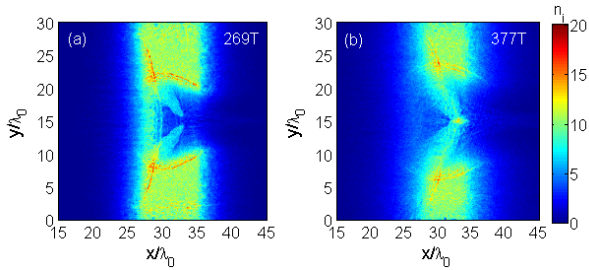


Figure 2: The density distributions of protons at  $t=269T$  (a) and  $t=377T$  (b) for the target with angles of  $60^\circ$ , in units of  $n_c$ . Other parameters are the same as that in the Fig.1.

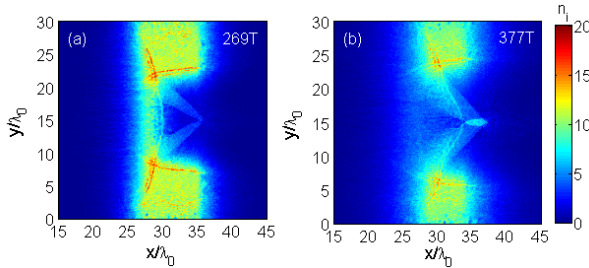


Figure 3: The density distributions of protons at  $t=269T$  (a) and  $t=377T$  (b) for the target with angles of  $120^\circ$ , in units of  $n_c$ . Other parameters are the same as that in the Fig.1.

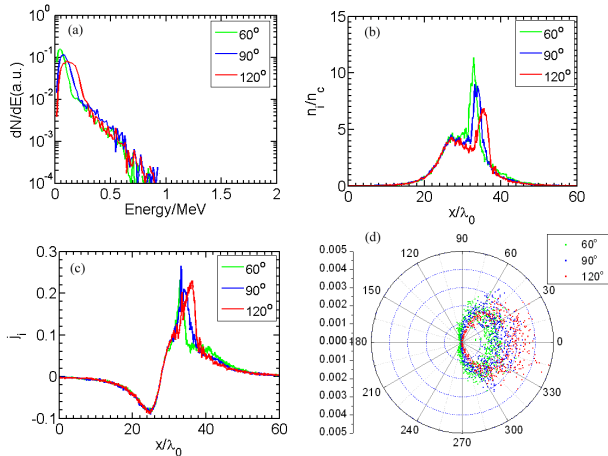


Figure 4: Energy spectra (a) and angular distributions (d) of the protons in the hole for the target of angles  $60^\circ$  (green line (points)),  $90^\circ$  (blue line (points)), and  $120^\circ$  (red line (points)) at  $t=377T$ , respectively. The density (b) and current density (c) distributions of the protons along the laser axis for the targets with angles  $60^\circ$  (green line),  $90^\circ$  (blue line), and  $120^\circ$  (red line) at  $t=377T$ , respectively, the current density is in unit of  $4.65 \times 10^{12} A/cm^2$ .

### CONCLUSION

We have presented a scheme to obtain collimated electron and proton bunch from the ultra-intense laser pulse interaction with a rear hole target. Energetic electron and proton jets are generated from the inner hole corners and merge on the laser axis, so a collimated plasma bunch is

produced and propagate in the hole along the laser axis without divergence. It is shown that the jets are emitted almost along the bisector of the corner angle and the latter is crucial to the quality of the proton bunch.

### REFERENCES

- [1] M. Kaluza, J. Schreiber, M. I. K. Santala, et al., Phys. Rev. Lett. 93 (2004) 045003.
- [2] H. Schworer, S. Pfoth, O. Jachkel, et al., Nature (London), 439 (2006) 445.
- [3] Y. Y. Ma, Z. M. Sheng, Y. Q. Gu, et al., Phys. Plasmas 16 (2009) 034502.
- [4] E. L. Clark, K. Krushelnick, J. R. Davies, et al., Phys. Rev. Lett. 84 (2000) 670.
- [5] M. Tabak, J. Hammer, M. E. Glinsky, et al., Phys. Plasmas 1 (1994) 1626.
- [6] B. A. Remington, D. Arnet, R. P. Drake, et al., Science 284 (1999) 1488.
- [7] K. W. D. Ledingham, P. McKenna, and R. P. Singhal, Science 300 (2003) 1107.
- [8] S. C. Wilks, A. B. Langdon, T. E. Cowan, et al., Phys. Plasmas 8 (2001) 542.
- [9] R. Sonobe, S. Kawata, S. Miyazaki, et al., Phys. Plasmas 12 (2005) 073104.
- [10] M. Nakamura, S. Kawata, R. Sonobe, et al., J. Appl. Phys. 101 (2007) 113305.
- [11] T. Toncian, M. Borghesi, J. Fuchs, et al., Science 312 (2006) 410.
- [12] Y. Y. Ma, Z. M. Sheng, Y. T. Li, et al., Phys. Plasmas 13 (2006) 110702.
- [13] G. Birkhoff, D. P. MacDougall, E. M. Pugh, et al., J. Appl. Phys. 19 (1948) 563.